Extended Data

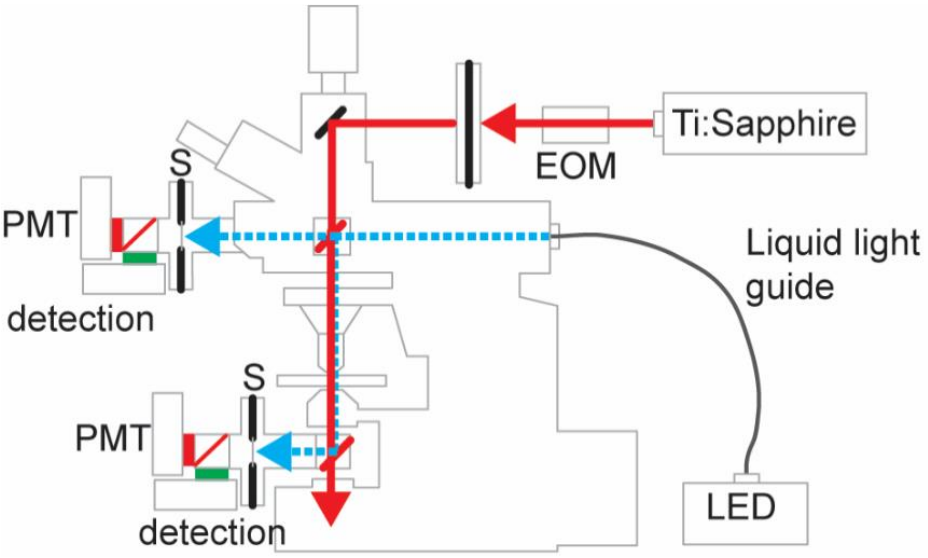

Extended Data Figure 1: Representation of imaging setup. A Ti:Sapphire laser system with dispersion compensation is coupled in through an electro-optical modulator (EOM). Red and green fluorescence is detected through the objective and through the oil immersion condenser (NA 1.4) using two pairs of photomultiplier tubes. 560 DXCR dichroic mirrors and 525/50 and 607/70 emission filters are used to separate green and red fluorescence. Excitation light is blocked by short-pass filters. A high-power LED coupled in through the epifluorescence port excites the red morphological marker allowing visualization of the transfected cells. During epifluorescence illumination, PMTs are protected by mechanical shutters (S).

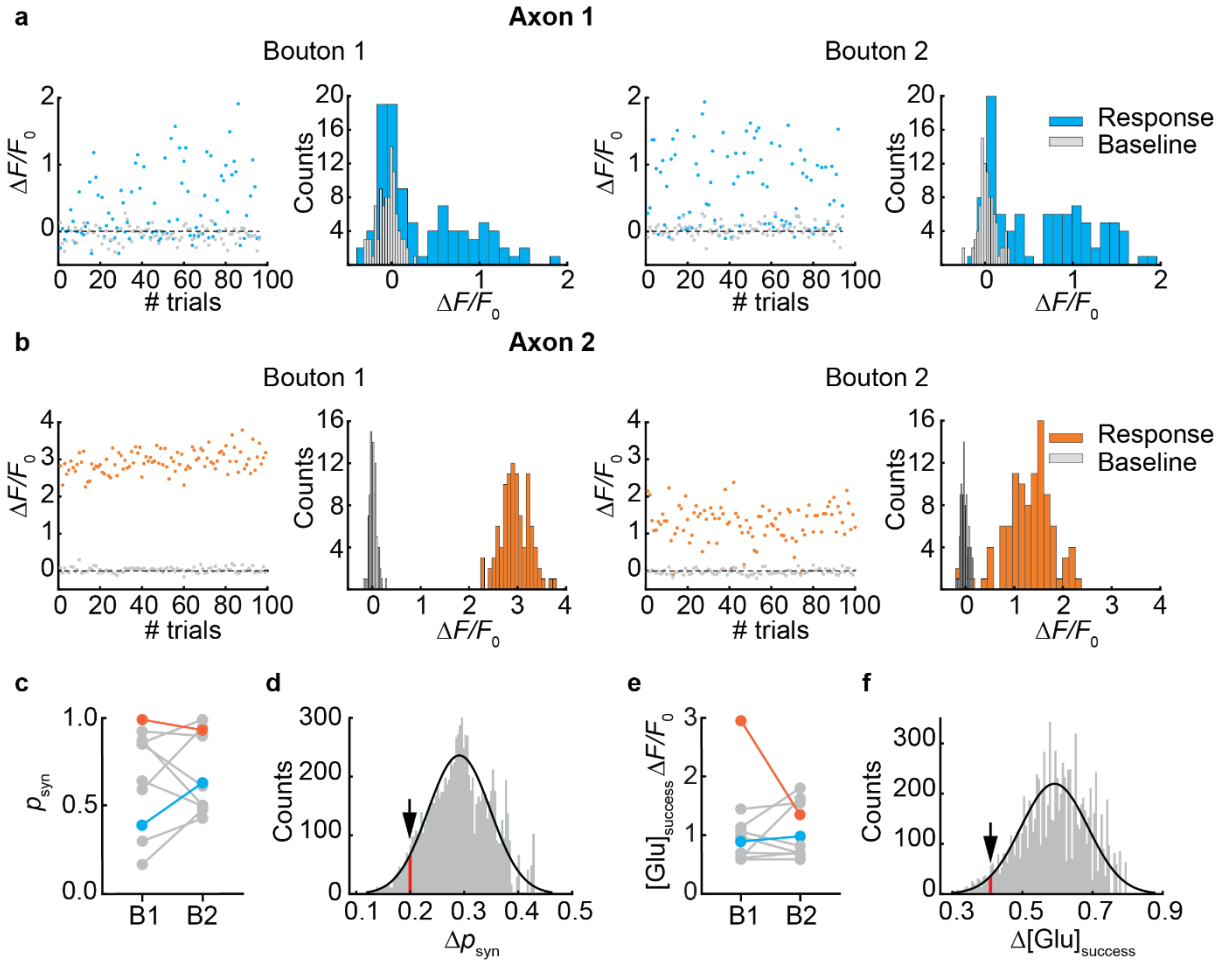

Extended Data Figure 2: Neighboring boutons show independent release properties.
a) Glutamate transients (blue dots) and baseline fluorescence (gray dots) of two neighboring boutons located on the same axon measured in ACSF containing 2 mM $[Ca^{2+}]_e$ *(left panels)* and their corresponding histogram counts (*right panels*). **b)** Same than in (**a**) for another pair of neighboring boutons. **c)** Synaptic release probability (p_{syn}) (calculated out of ~100 trials) of individual boutons (B1) and their neighboring bouton on the same axon (B2); n = 10 pairs of boutons in 9 slices. The pair of neighboring boutons from (**a)** and (**b**) is shown in blue and orange, respectively. **d)** Histogram of $\Delta p_{syn} = |p_{syn}$ BX $- p_{syn}$ BY$|$. BX and BY are randomly paired from the dataset in c. The measured difference in p_{syn}, $|p_{syn}$ B2 $- p_{syn}$ B1$|$ (black arrow), is not significantly smaller than the mean Δp_{syn} of two boutons from the dataset paired randomly (grey bars) (p = 0.053). **e)** Cleft glutamate of a given bouton (B1) and its direct neighbor located on the same axon (B2); n = 10 pairs of boutons in 9 slices. The pairs of neighboring boutons from (**a**) and (**b**) are shown in blue and orange, respectively. **f)** The average difference of cleft glutamate ($\Delta F/F_0$) of successes between two neighboring boutons (black arrow) is significantly different (p = 0.027) from the average difference when boutons are connected randomly (grey bars).

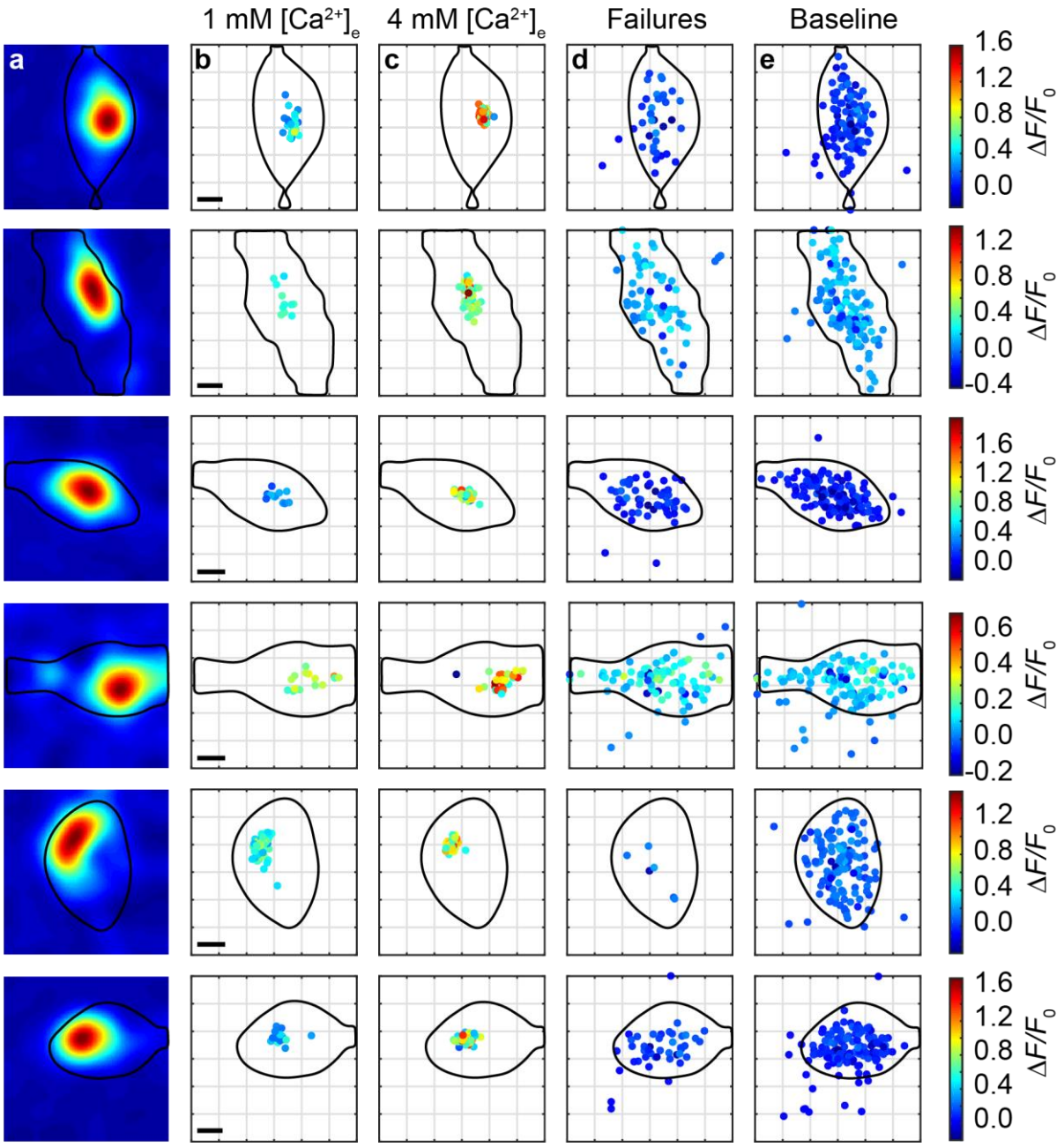

Extended Data Figure 3: Localization of fluorescence transients under high and low release probability. a) Average response of iGluSnFR superimposed with bouton outline (black line). **b**) Fusion appears to be localized to a small region on the bouton (active zone). Amplitude ($\Delta F/F_0$) of individual trials is color-coded. **c)** Increasing the extracellular calcium concentration increased the amplitude of individual responses but did not lead to release events outside the active zone. **d)** Fitting responses classified as failures (< 2σ of baseline) did not reveal any clustering, indicating that there was indeed no localized signal (true negatives). **e)** Fitting baseline iGluSnFR fluorescence did not result in clustering. Scale bar, 0.5 µm.

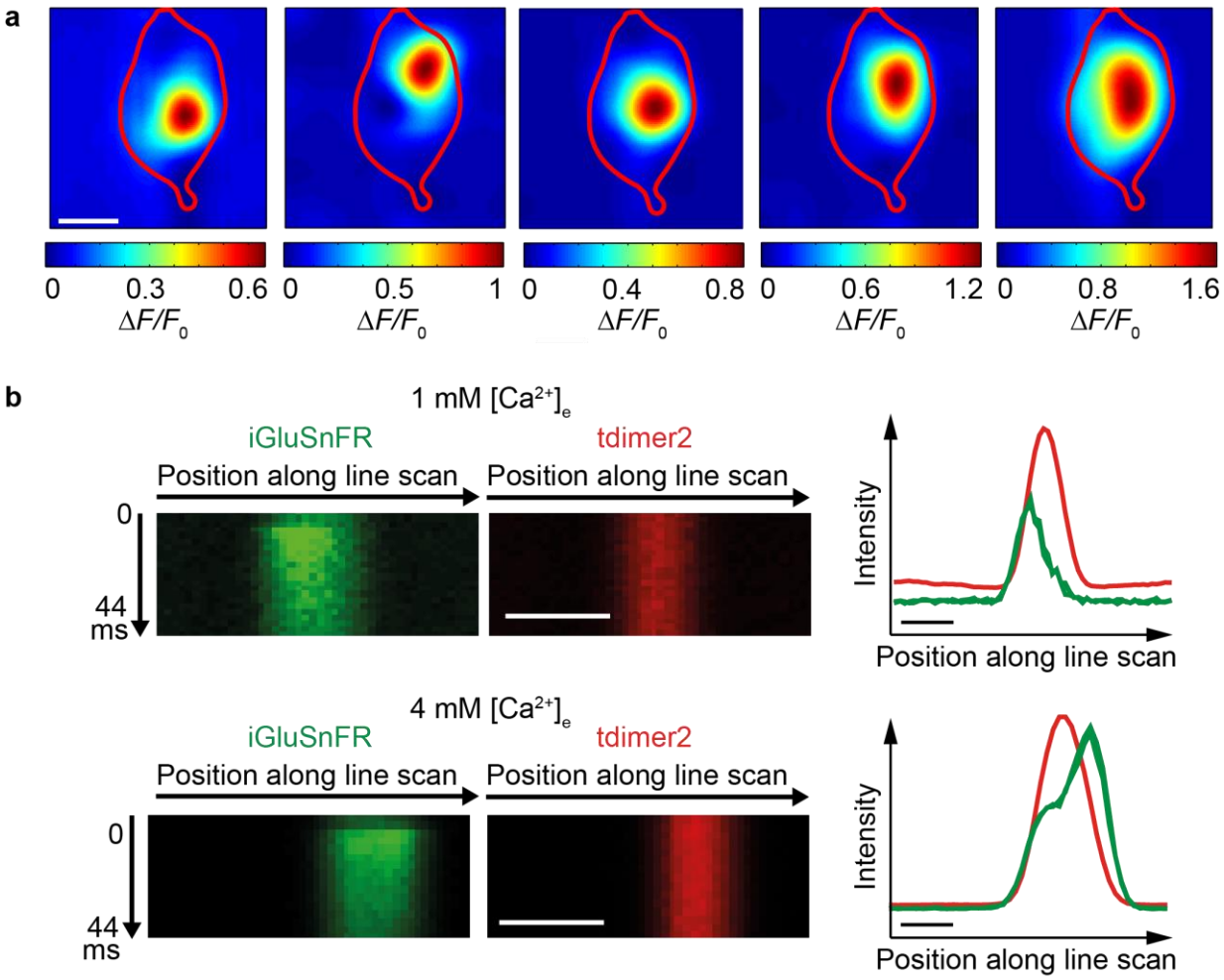

Extended Data Figure 4: Multisynaptic boutons show a second release site under high release probability. a) Example of color-coded iGluSnFR signal of a multi-synapse bouton. Each frame represent the iGluSnFR signal in response to a single action potential in a given bouton. Scale bar,1 µm. **b)** Example of the average intensity profile (average of ~ 30 trials) *post hoc* aligned on the red morphological marker of a straight line scan across a multisynaptic bouton in 1 mM $[Ca^{2+}]_e$ (*upper panel*) with a single hot spot and in 4 mM $[Ca^{2+}]_e$ (*lower panel*) with the appearance of a second hot spot. All boutons with a similar pattern of release were excluded from further analysis. Scale bar, 1 µm.

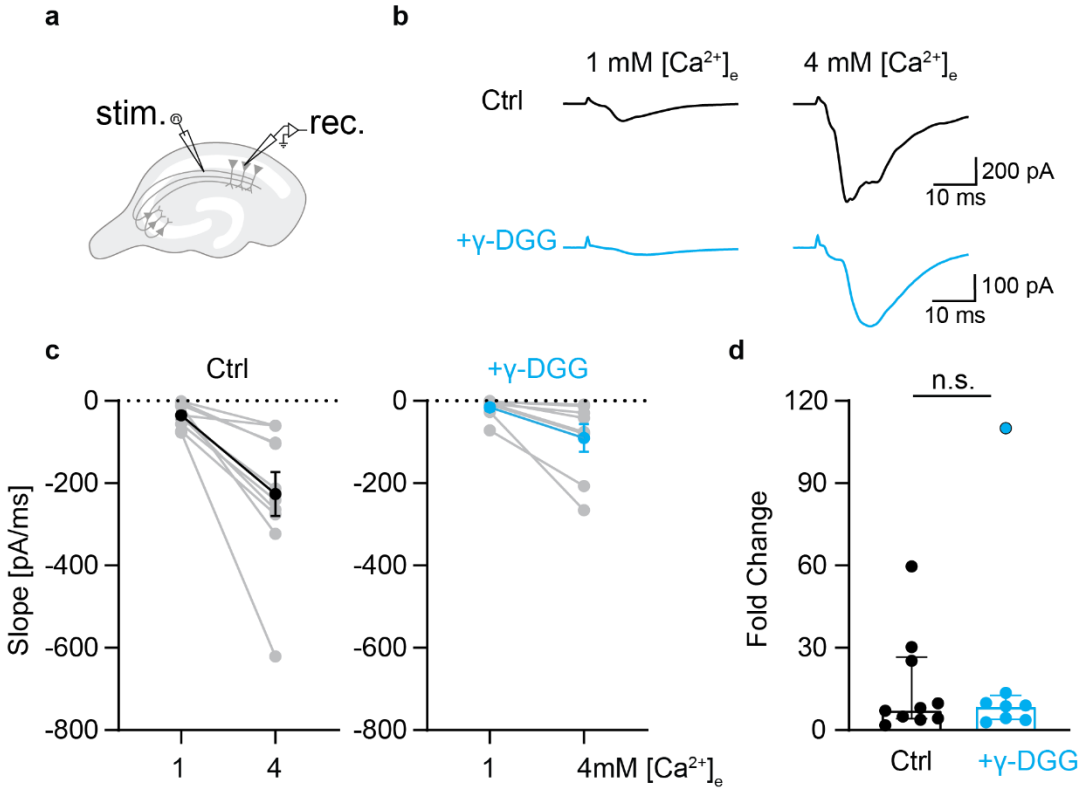

Extended Data Figure 5: Low occupancy of AMPARs. a) A monopolar electrode placed in *stratum radiatum* was used to elicit postsynaptic responses measured in whole cell voltage clamp from a CA1 neuron located ~300 µm away. To isolate AMPARs, the NMDAR blocker CPP-ene (10 µM) was added to the bath. **b)** Example traces of AMPARs responses measured in response to electrical filed stimulation in control condition *(upper traces)* and upon addition of 10 mM γ-DGG, a competitive AMPARs antagonist *(lower traces)* which led to decreased evoked EPSCs. **c)** *(Left panel)* Slope measurements of evoked EPSCs in control condition in 1 mM $[Ca^{2+}]_e$: -35.1 ± 8.8 pA/ms and in 4 mM $[Ca^{2+}]_e$: -226.5 ± 53.2 pA/ms, *n* = 10 cells. *(Right panel)* Slope measurements upon application of γ-DGG in 1 mM $[Ca^{2+}]_e$: -15.5 ± 8.5 pA/ms and in 4 mM $[Ca^{2+}]_e$: -90.1 ± 33.7 pA/ms, *n* = 8 cells. Values are plotted as mean ± SEM. **d)** Decrease of AMPARs occupancy did not lead to a significant increase in postsynaptic fold change from low to high $[Ca^{2+}]_e$. There is no significant fold change from 1 mM to 4 mM $[Ca^{2+}]_e$ in the absence (median: 7.57 fold, IQR: 4.1–26.5 fold, *n* = 10 cells) or presence of γ-DGG (median: 8.84 fold, IQR: 3.8–12.6 fold, *n* = 8 cells) (Mann Whitney test, *p* = 0.97). Values are plotted as median with IQR.

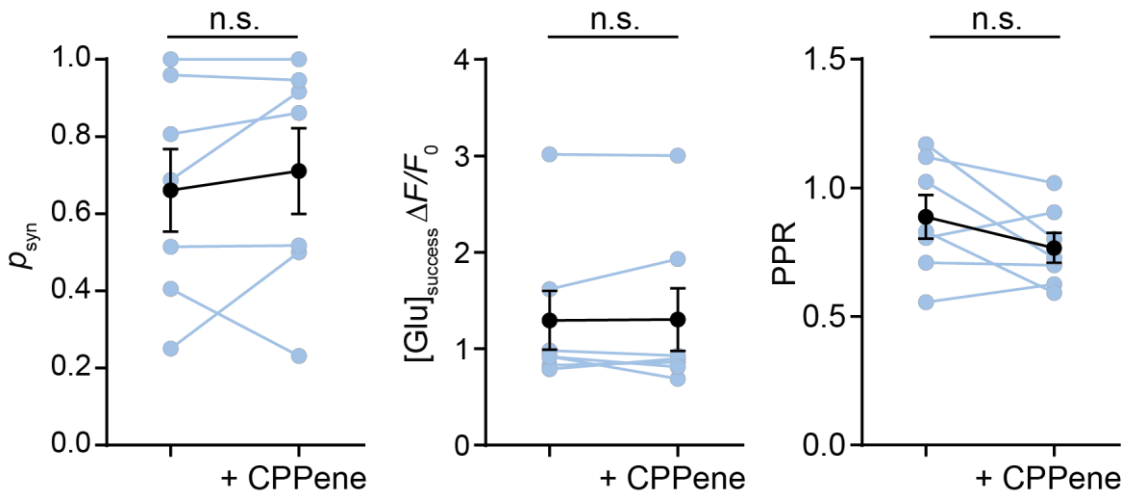

Extended Data Figure 6: Unchanged synaptic release probability upon block of NMDAR. iGluSnFR changes in fluorescence (single bouton, ~30 consecutive trials) were measured in response to single action potentials before and after the application of the NMDARs blocker CPPene (10 µM). There was no significant difference under NMDARs block in synaptic release probability, Ctrl: 0.66 ± 0.1, NMDAR block: 0.71 ± 0.1, paired t-test, p = 0.41; cleft glutamate, Ctrl: 1.3 ± 0.3 $\Delta F/F_0$, NMDAR block: 1.3 ± 0.3 $\Delta F/F_0$, Wilcoxon test, p = 0.94; and PPR, Ctrl: 89% ± 9%, NMDAR block: 77% ± 6%, paired t-test, p = 0.13; n = 7 boutons in 7 slices. Values are plotted as mean ± SEM.

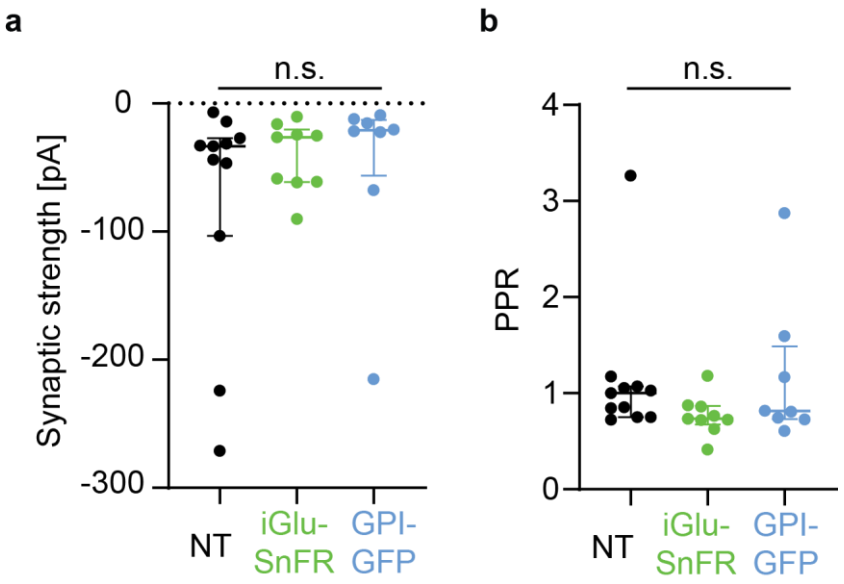

Extended Data Figure 7: Expression of iGluSnFR does not affect synaptic transmission. a) EPSCs were measured by dual patch-clamp recordings from connected CA3-CA1 pyramidal cell pairs in 4 mM $[Ca^{2+}]_e$. The NMDA blocker CPPene (10 µM) was added to the bath to isolate AMPARs reponses. EPSCs were recorded from non-transfected (NT) CA3-CA1 pairs (median synaptic strength: -33.4 pA, IQR: -103.3 – -27.2 pA, *n* = 11 pairs); iGluSnFR-expressing CA3-CA1 pairs (median synaptic strength: -26.4 pA, IQR: -61.4 – -20.25 pA, *n* = 9 pairs); GPI-GFP-expressing CA3-CA1 pairs (median synaptic strength: -21.0 pA, IQR: -56.2 – -12.9 pA, *n* = 8 pairs). There was no significant difference in measured synaptic strength between the different groups of connected CA3-CA1 pairs (Kruskal-Wallis test, *p* = 0.31). **b)** EPSCs showed paired-pulse depression (ISI = 48 ms) in 4 mM $[Ca^{2+}]_e$ for NT CA3-CA1 pairs (median PPR: 100%, IQR: 75% – 107%, *n* = 11 pairs), for the iGluSnFR expressing CA3-CA1 (median PPR: 74%, IQR: 68% – 87%, *n* = 9 pairs) and for the GPI-GFP CA3 expressing-CA1 pairs (median PPR: 81%, IQR: 73%– 149%, *n* = 8 pairs). There was no significant difference in measured synaptic strength between the different groups of connected CA3-CA1 pairs (Kruskal-Wallis test, *p* = 0.17). Values are plotted as median with IQR.

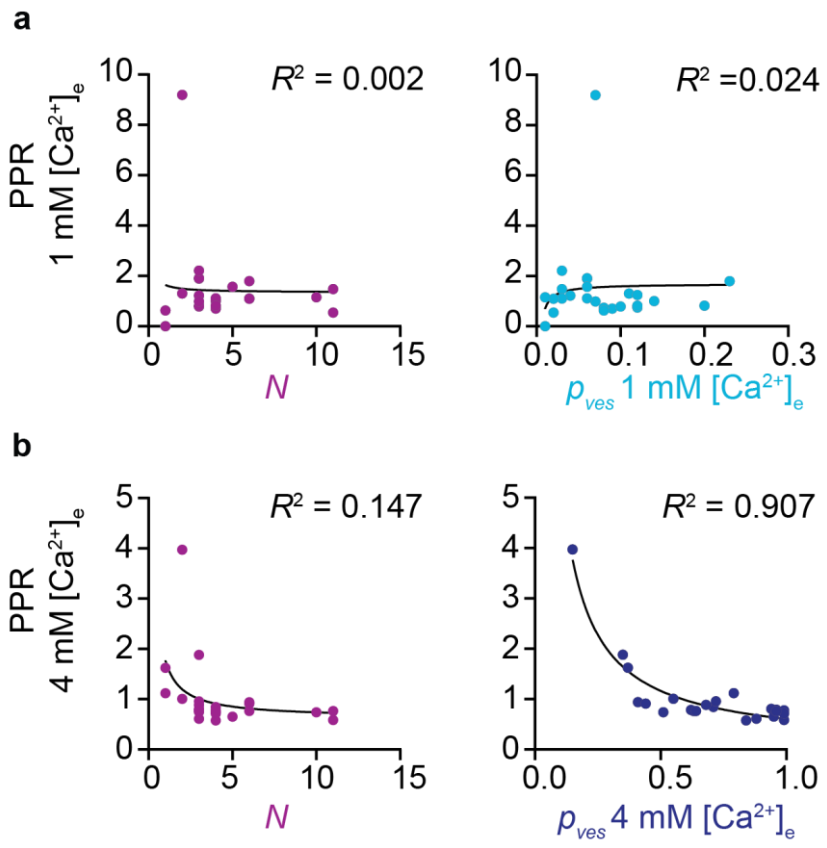

Extended Data Figure 8: Hetereogeneous PPR as a function of quantal parameters.
a) PPR in 1 mM $[Ca^{2+}]_e$ as a function of *N* and p_{ves} in 1 mM $[Ca^{2+}]_e$ (*n* = 25 boutons). Coefficients of determination were determined by fitting hyperbolic functions (y = (a/x) + b).
b) PPR in 4 mM $[Ca^{2+}]_e$ as a function of *N* and p_{ves} in 4 mM $[Ca^{2+}]_e$ (*n* = 25 boutons). Coefficients of determination were determined by fitting hyperbolic functions.

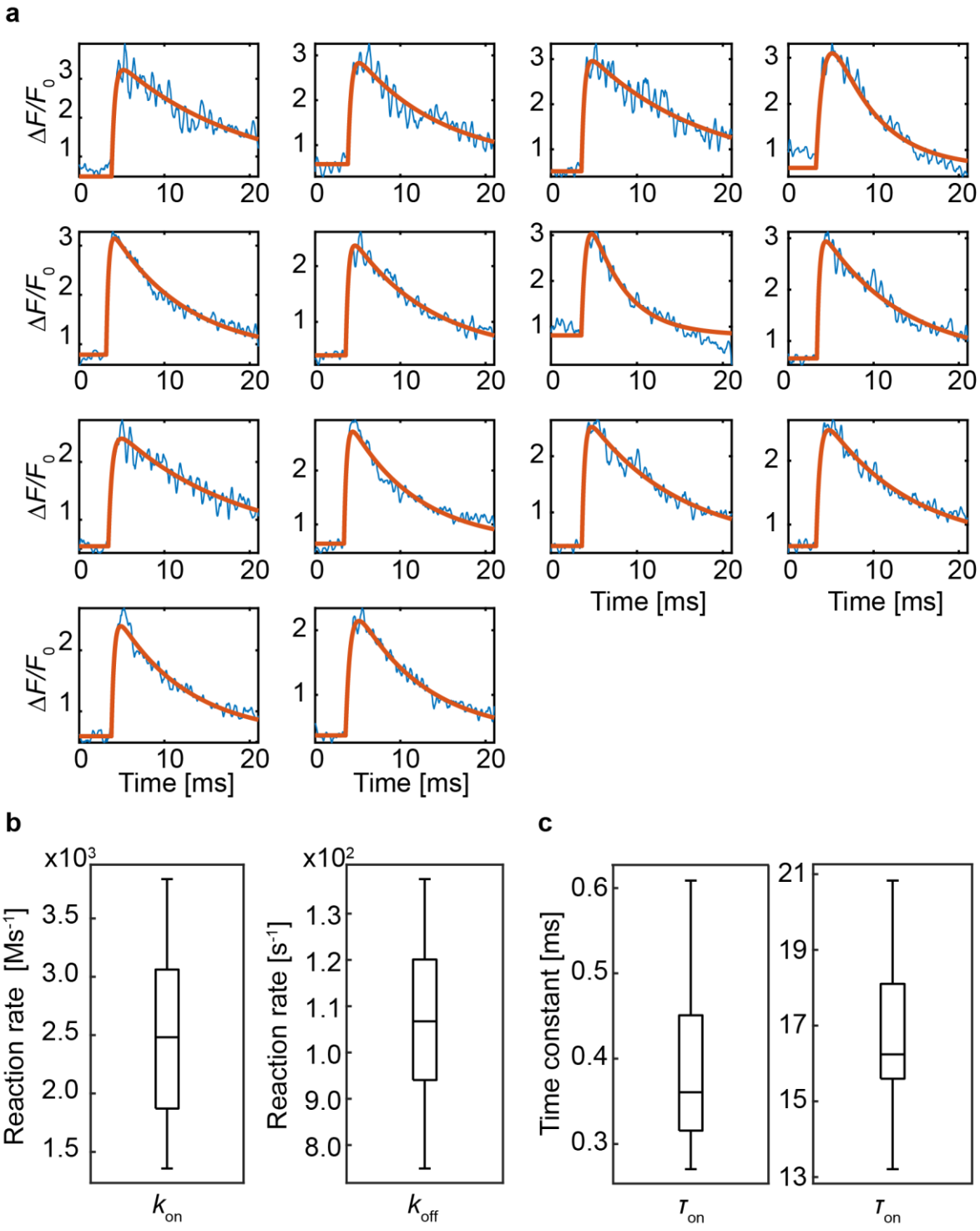

Extended Data Figure 9: iGluSnFR kinetics from synaptic imaging data. a) Example traces of point scan at 1 kHz of iGluSnFR signal in response to a single AP fitted with a double exponential **b)** Reaction rates, k_{on}: 2481 Ms^{-1}, k_{off} : 111 s^{-1} **c)** Time constants, τ_{on} : 4.8 ms, τ_{off} : 16.1 ms.